

# Pion, kaon, proton and anti-proton transverse momentum distributions from p+p and d+Au collisions at $\sqrt{s_{NN}} = 200$ GeV

J. Adams,<sup>3</sup> M.M. Aggarwal,<sup>29</sup> Z. Ahammed,<sup>43</sup> J. Amonett,<sup>20</sup> B.D. Anderson,<sup>20</sup> D. Arkhipkin,<sup>13</sup> G.S. Averichev,<sup>12</sup> S.K. Badyal,<sup>19</sup> Y. Bai,<sup>27</sup> J. Balewski,<sup>17</sup> O. Barannikova,<sup>32</sup> L.S. Barnby,<sup>3</sup> J. Baudot,<sup>18</sup> S. Bekele,<sup>28</sup> V.V. Belaga,<sup>12</sup> R. Bellwied,<sup>46</sup> J. Berger,<sup>14</sup> B.I. Bezverkhny,<sup>48</sup> S. Bharadwaj,<sup>33</sup> A. Bhasin,<sup>19</sup> A.K. Bhati,<sup>29</sup> V.S. Bhatia,<sup>29</sup> H. Bichsel,<sup>45</sup> J. Bielcik,<sup>48</sup> J. Bielcikova,<sup>48</sup> A. Billmeier,<sup>46</sup> L.C. Bland,<sup>4</sup> C.O. Blyth,<sup>3</sup> B.E. Bonner,<sup>34</sup> M. Botje,<sup>27</sup> A. Boucham,<sup>38</sup> A.V. Brandin,<sup>25</sup> A. Bravar,<sup>4</sup> M. Bystersky,<sup>11</sup> R.V. Cadman,<sup>1</sup> X.Z. Cai,<sup>37</sup> H. Caines,<sup>48</sup> M. Calderón de la Barca Sánchez,<sup>17</sup> J. Castillo,<sup>21</sup> O. Catu,<sup>48</sup> D. Cebra,<sup>7</sup> Z. Chajecki,<sup>44</sup> P. Chaloupka,<sup>11</sup> S. Chattopadhyay,<sup>43</sup> H.F. Chen,<sup>36</sup> Y. Chen,<sup>8</sup> J. Cheng,<sup>41</sup> M. Cherney,<sup>10</sup> A. Chikianian,<sup>48</sup> W. Christie,<sup>4</sup> J.P. Coffin,<sup>18</sup> T.M. Cormier,<sup>46</sup> J.G. Cramer,<sup>45</sup> H.J. Crawford,<sup>6</sup> D. Das,<sup>43</sup> S. Das,<sup>43</sup> M.M. de Moura,<sup>35</sup> A.A. Derevschikov,<sup>31</sup> L. Didenko,<sup>4</sup> T. Dietel,<sup>14</sup> S.M. Dogra,<sup>19</sup> W.J. Dong,<sup>8</sup> X. Dong,<sup>36</sup> J.E. Draper,<sup>7</sup> F. Du,<sup>48</sup> A.K. Dubey,<sup>15</sup> V.B. Dunin,<sup>12</sup> J.C. Dunlop,<sup>4</sup> M.R. Dutta Mazumdar,<sup>43</sup> V. Eckardt,<sup>23</sup> W.R. Edwards,<sup>21</sup> L.G. Efimov,<sup>12</sup> V. Emelianov,<sup>25</sup> J. Engelage,<sup>6</sup> G. Eppley,<sup>34</sup> B. Erazmus,<sup>38</sup> M. Estienne,<sup>38</sup> P. Fachini,<sup>4</sup> J. Faivre,<sup>18</sup> R. Fatemi,<sup>17</sup> J. Fedorisin,<sup>12</sup> K. Filimonov,<sup>21</sup> P. Filip,<sup>11</sup> E. Finch,<sup>48</sup> V. Fine,<sup>4</sup> Y. Fisyak,<sup>4</sup> K. Fomenko,<sup>12</sup> J. Fu,<sup>41</sup> C.A. Gagliardi,<sup>39</sup> L. Gaillard,<sup>3</sup> J. Gans,<sup>48</sup> M.S. Ganti,<sup>43</sup> L. Gaudichet,<sup>38</sup> F. Geurts,<sup>34</sup> V. Ghazikhanian,<sup>8</sup> P. Ghosh,<sup>43</sup> J.E. Gonzalez,<sup>8</sup> O. Grachov,<sup>46</sup> O. Grebenyuk,<sup>27</sup> D. Grosnick,<sup>42</sup> S.M. Guertin,<sup>8</sup> Y. Guo,<sup>46</sup> A. Gupta,<sup>19</sup> T.D. Gutierrez,<sup>7</sup> T.J. Hallman,<sup>4</sup> A. Hamed,<sup>46</sup> D. Hardtke,<sup>21</sup> J.W. Harris,<sup>48</sup> M. Heinz,<sup>2</sup> T.W. Henry,<sup>39</sup> S. Hepplemann,<sup>30</sup> B. Hippolyte,<sup>18</sup> A. Hirsch,<sup>32</sup> E. Hjort,<sup>21</sup> G.W. Hoffmann,<sup>40</sup> H.Z. Huang,<sup>8</sup> S.L. Huang,<sup>36</sup> E.W. Hughes,<sup>5</sup> T.J. Humanic,<sup>28</sup> G. Igo,<sup>8</sup> A. Ishihara,<sup>40</sup> P. Jacobs,<sup>21</sup> W.W. Jacobs,<sup>17</sup> M. Janik,<sup>44</sup> H. Jiang,<sup>8</sup> P.G. Jones,<sup>3</sup> E.G. Judd,<sup>6</sup> S. Kabana,<sup>2</sup> K. Kang,<sup>41</sup> M. Kaplan,<sup>9</sup> D. Keane,<sup>20</sup> V.Yu. Khodyrev,<sup>31</sup> J. Kiryluk,<sup>22</sup> A. Kisiel,<sup>44</sup> E.M. Kislov,<sup>12</sup> J. Klay,<sup>21</sup> S.R. Klein,<sup>21</sup> D.D. Koetke,<sup>42</sup> T. Kollegger,<sup>14</sup> M. Kopytine,<sup>20</sup> L. Kotchenda,<sup>25</sup> M. Kramer,<sup>26</sup> P. Kravtsov,<sup>25</sup> V.I. Kravtsov,<sup>31</sup> K. Krueger,<sup>1</sup> C. Kuhn,<sup>18</sup> A.I. Kulikov,<sup>12</sup> A. Kumar,<sup>29</sup> R.Kh. Kutuev,<sup>13</sup> A.A. Kuznetsov,<sup>12</sup> M.A.C. Lamont,<sup>48</sup> J.M. Landgraf,<sup>4</sup> S. Lange,<sup>14</sup> F. Laue,<sup>4</sup> J. Lauret,<sup>4</sup> A. Lebedev,<sup>4</sup> R. Lednicky,<sup>12</sup> S. Lehocka,<sup>12</sup> M.J. LeVine,<sup>4</sup> C. Li,<sup>36</sup> Q. Li,<sup>46</sup> Y. Li,<sup>41</sup> G. Lin,<sup>48</sup> S.J. Lindenbaum,<sup>26</sup> M.A. Lisa,<sup>28</sup> F. Liu,<sup>47</sup> L. Liu,<sup>47</sup> Q.J. Liu,<sup>45</sup> Z. Liu,<sup>47</sup> T. Ljubicic,<sup>4</sup> W.J. Llope,<sup>34</sup> H. Long,<sup>8</sup> R.S. Longacre,<sup>4</sup> M. Lopez-Noriega,<sup>28</sup> W.A. Love,<sup>4</sup> Y. Lu,<sup>47</sup> T. Ludlam,<sup>4</sup> D. Lynn,<sup>4</sup> G.L. Ma,<sup>37</sup> J.G. Ma,<sup>8</sup> Y.G. Ma,<sup>37</sup> D. Magestro,<sup>28</sup> S. Mahajan,<sup>19</sup> D.P. Mahapatra,<sup>15</sup> R. Majka,<sup>48</sup> L.K. Mangotra,<sup>19</sup> R. Manweiler,<sup>42</sup> S. Margetis,<sup>20</sup> C. Markert,<sup>20</sup> L. Martin,<sup>38</sup> J.N. Marx,<sup>21</sup> H.S. Matis,<sup>21</sup> Yu.A. Matulenko,<sup>31</sup> C.J. McClain,<sup>1</sup> T.S. McShane,<sup>10</sup> F. Meissner,<sup>21</sup> Yu. Melnick,<sup>31</sup> A. Meschanin,<sup>31</sup> M.L. Miller,<sup>22</sup> N.G. Minaev,<sup>31</sup> C. Mironov,<sup>20</sup> A. Mischke,<sup>27</sup> D.K. Mishra,<sup>15</sup> J. Mitchell,<sup>34</sup> B. Mohanty,<sup>43</sup> L. Molnar,<sup>32</sup> C.F. Moore,<sup>40</sup> D.A. Morozov,<sup>31</sup> M.G. Munhoz,<sup>35</sup> B.K. Nandi,<sup>43</sup> S.K. Nayak,<sup>19</sup> T.K. Nayak,<sup>43</sup> J.M. Nelson,<sup>3</sup> P.K. Netrakanti,<sup>43</sup> V.A. Nikitin,<sup>13</sup> L.V. Nogach,<sup>31</sup> S.B. Nurushev,<sup>31</sup> G. Odyniec,<sup>21</sup> A. Ogawa,<sup>4</sup> V. Okorokov,<sup>25</sup> M. Oldenburg,<sup>21</sup> D. Olson,<sup>21</sup> S.K. Pal,<sup>43</sup> Y. Panebratsev,<sup>12</sup> S.Y. Panitkin,<sup>4</sup> A.I. Pavlinov,<sup>46</sup> T. Pawlak,<sup>44</sup> T. Peitzmann,<sup>27</sup> V. Perevozchikov,<sup>4</sup> C. Perkins,<sup>6</sup> W. Peryt,<sup>44</sup> V.A. Petrov,<sup>13</sup> S.C. Phatak,<sup>15</sup> R. Picha,<sup>7</sup> M. Planinic,<sup>49</sup> J. Pluta,<sup>44</sup> N. Porile,<sup>32</sup> J. Porter,<sup>45</sup> A.M. Poskanzer,<sup>21</sup> M. Potekhin,<sup>4</sup> E. Potrebenikova,<sup>12</sup> B.V.K.S. Potukuchi,<sup>19</sup> D. Prindle,<sup>45</sup> C. Pruneau,<sup>46</sup> J. Putschke,<sup>23</sup> G. Rakness,<sup>30</sup> R. Raniwala,<sup>33</sup> S. Raniwala,<sup>33</sup> O. Ravel,<sup>38</sup> R.L. Ray,<sup>40</sup> S.V. Razin,<sup>12</sup> D. Reichhold,<sup>32</sup> J.G. Reid,<sup>45</sup> G. Renault,<sup>38</sup> F. Retiere,<sup>21</sup> A. Ridiger,<sup>25</sup> H.G. Ritter,<sup>21</sup> J.B. Roberts,<sup>34</sup> O.V. Rogachevskiy,<sup>12</sup> J.L. Romero,<sup>7</sup> A. Rose,<sup>46</sup> C. Roy,<sup>38</sup> L. Ruan,<sup>36</sup> R. Sahoo,<sup>15</sup> I. Sakrejda,<sup>21</sup> S. Salur,<sup>48</sup> J. Sandweiss,<sup>48</sup> M. Sarsour,<sup>17</sup> I. Savin,<sup>13</sup> P.S. Sazhin,<sup>12</sup> J. Schambach,<sup>40</sup> R.P. Scharenberg,<sup>32</sup> N. Schmitz,<sup>23</sup> K. Schweda,<sup>21</sup> J. Seger,<sup>10</sup> P. Seyboth,<sup>23</sup> E. Shahaliev,<sup>12</sup> M. Shao,<sup>36</sup> W. Shao,<sup>5</sup> M. Sharma,<sup>29</sup> W.Q. Shen,<sup>37</sup> K.E. Shestermanov,<sup>31</sup> S.S. Shimanskiy,<sup>12</sup> E. Sichtermann,<sup>21</sup> F. Simon,<sup>23</sup> R.N. Singaraju,<sup>43</sup> G. Skoro,<sup>12</sup> N. Smirnov,<sup>48</sup> R. Snellings,<sup>27</sup> G. Sood,<sup>42</sup> P. Sorensen,<sup>21</sup> J. Sowinski,<sup>17</sup> J. Speltz,<sup>18</sup> H.M. Spinka,<sup>1</sup> B. Srivastava,<sup>32</sup> A. Stadnik,<sup>12</sup> T.D.S. Stanislaus,<sup>42</sup> R. Stock,<sup>14</sup> A. Stolpovsky,<sup>46</sup> M. Strikhanov,<sup>25</sup> B. Stringfellow,<sup>32</sup> A.A.P. Suade,<sup>35</sup> E. Sugarbaker,<sup>28</sup> C. Suire,<sup>4</sup> M. Sumbera,<sup>11</sup> B. Surrow,<sup>22</sup> T.J.M. Symons,<sup>21</sup> A. Szanto de Toledo,<sup>35</sup> P. Szarwas,<sup>44</sup> A. Tai,<sup>8</sup> J. Takahashi,<sup>35</sup> A.H. Tang,<sup>27</sup> T. Tarnowsky,<sup>32</sup> D. Thein,<sup>8</sup> J.H. Thomas,<sup>21</sup> S. Timoshenko,<sup>25</sup> M. Tokarev,<sup>12</sup> T.A. Trainor,<sup>45</sup> S. Trentalange,<sup>8</sup> R.E. Tribble,<sup>39</sup> O.D. Tsai,<sup>8</sup> J. Ulery,<sup>32</sup> T. Ullrich,<sup>4</sup> D.G. Underwood,<sup>1</sup> A. Urkinbaev,<sup>12</sup> G. Van Buren,<sup>4</sup> M. van Leeuwen,<sup>21</sup> A.M. Vander Molen,<sup>24</sup> R. Varma,<sup>16</sup> I.M. Vasilevski,<sup>13</sup> A.N. Vasiliev,<sup>31</sup> R. Vernet,<sup>18</sup> S.E. Vigdor,<sup>17</sup> Y.P. Viyogi,<sup>43</sup> S. Vokal,<sup>12</sup> S.A. Voloshin,<sup>46</sup> M. Vznuzdaev,<sup>25</sup> W.T. Waggoner,<sup>10</sup> F. Wang,<sup>32</sup> G. Wang,<sup>20</sup> G. Wang,<sup>5</sup> X.L. Wang,<sup>36</sup> Y. Wang,<sup>40</sup> Y. Wang,<sup>41</sup> Z.M. Wang,<sup>36</sup> H. Ward,<sup>40</sup> J.W. Watson,<sup>20</sup> J.C. Webb,<sup>17</sup> R. Wells,<sup>28</sup> G.D. Westfall,<sup>24</sup> A. Wetzler,<sup>21</sup> C. Whitten Jr.,<sup>8</sup> H. Wieman,<sup>21</sup> S.W. Wissink,<sup>17</sup> R. Witt,<sup>2</sup> J. Wood,<sup>8</sup> J. Wu,<sup>36</sup> N. Xu,<sup>21</sup> Z. Xu,<sup>4</sup> Z.Z. Xu,<sup>36</sup> E. Yamamoto,<sup>21</sup> P. Yepes,<sup>34</sup> V.I. Yurevich,<sup>12</sup> Y.V. Zanevsky,<sup>12</sup> H. Zhang,<sup>4</sup> W.M. Zhang,<sup>20</sup> Z.P. Zhang,<sup>36</sup> R. Zoukarneeva,<sup>13</sup> Y. Zoukarneeva,<sup>13</sup> and A.N. Zubarev<sup>12</sup>

## (STAR Collaboration), \*

<sup>1</sup> Argonne National Laboratory, Argonne, Illinois 60439<sup>2</sup> University of Bern, 3012 Bern, Switzerland<sup>3</sup> University of Birmingham, Birmingham, United Kingdom<sup>4</sup> Brookhaven National Laboratory, Upton, New York 11973<sup>5</sup> California Institute of Technology, Pasadena, California 91125<sup>6</sup> University of California, Berkeley, California 94720<sup>7</sup> University of California, Davis, California 95616<sup>8</sup> University of California, Los Angeles, California 90095<sup>9</sup> Carnegie Mellon University, Pittsburgh, Pennsylvania 15213<sup>10</sup> Creighton University, Omaha, Nebraska 68178<sup>11</sup> Nuclear Physics Institute AS CR, 250 68 Řež/Prague, Czech Republic<sup>12</sup> Laboratory for High Energy (JINR), Dubna, Russia<sup>13</sup> Particle Physics Laboratory (JINR), Dubna, Russia<sup>14</sup> University of Frankfurt, Frankfurt, Germany<sup>15</sup> Institute of Physics, Bhubaneswar 751005, India<sup>16</sup> Indian Institute of Technology, Mumbai, India<sup>17</sup> Indiana University, Bloomington, Indiana 47408<sup>18</sup> Institut de Recherches Subatomiques, Strasbourg, France<sup>19</sup> University of Jammu, Jammu 180001, India<sup>20</sup> Kent State University, Kent, Ohio 44242<sup>21</sup> Lawrence Berkeley National Laboratory, Berkeley, California 94720<sup>22</sup> Massachusetts Institute of Technology, Cambridge, MA 02139-4307<sup>23</sup> Max-Planck-Institut für Physik, Munich, Germany<sup>24</sup> Michigan State University, East Lansing, Michigan 48824<sup>25</sup> Moscow Engineering Physics Institute, Moscow Russia<sup>26</sup> City College of New York, New York City, New York 10031<sup>27</sup> NIKHEF, Amsterdam, The Netherlands<sup>28</sup> Ohio State University, Columbus, Ohio 43210<sup>29</sup> Panjab University, Chandigarh 160014, India<sup>30</sup> Pennsylvania State University, University Park, Pennsylvania 16802<sup>31</sup> Institute of High Energy Physics, Protvino, Russia<sup>32</sup> Purdue University, West Lafayette, Indiana 47907<sup>33</sup> University of Rajasthan, Jaipur 302004, India<sup>34</sup> Rice University, Houston, Texas 77251<sup>35</sup> Universidade de São Paulo, São Paulo, Brazil<sup>36</sup> University of Science & Technology of China, Anhui 230027, China<sup>37</sup> Shanghai Institute of Applied Physics, Shanghai 201800, China<sup>38</sup> SUBATECH, Nantes, France<sup>39</sup> Texas A&M University, College Station, Texas 77843<sup>40</sup> University of Texas, Austin, Texas 78712<sup>41</sup> Tsinghua University, Beijing 100084, China<sup>42</sup> Valparaiso University, Valparaiso, Indiana 46383<sup>43</sup> Variable Energy Cyclotron Centre, Kolkata 700064, India<sup>44</sup> Warsaw University of Technology, Warsaw, Poland<sup>45</sup> University of Washington, Seattle, Washington 98195<sup>46</sup> Wayne State University, Detroit, Michigan 48201<sup>47</sup> Institute of Particle Physics, CCNU (HZNU), Wuhan 430079, China<sup>48</sup> Yale University, New Haven, Connecticut 06520<sup>49</sup> University of Zagreb, Zagreb, HR-10002, Croatia

(Dated: February 9, 2020)

Identified mid-rapidity particle spectra of  $\pi^\pm$ ,  $K^\pm$ , and  $p(\bar{p})$  from 200 GeV p+p and d+Au collisions are reported. A time-of-flight detector based on multi-gap resistive plate chamber technology is used for particle identification. The particle-species dependence of the Cronin effect is observed to be significantly smaller than that at lower energies. The ratio of the nuclear modification factor ( $R_{dAu}$ ) between protons ( $p + \bar{p}$ ) and charged hadrons ( $h$ ) in the transverse momentum range  $1.2 < p_T < 3.0$  GeV/c is measured to be  $1.19 \pm 0.05(\text{stat}) \pm 0.03(\text{syst})$  in minimum-bias collisions and shows little centrality dependence. The yield ratio of  $(p + \bar{p})/h$  in minimum-bias d+Au collisions is found to be a factor of 2 lower than that in Au+Au collisions, indicating that the Cronin effect alone is not enough to account for the relative baryon enhancement observed in heavy ion collisions at RHIC.

Suppression of high transverse momentum ( $p_T$ ) hadron production has been observed at RHIC in central Au+Au collisions relative to p+p collisions [1, 2, 3, 4]. This suppression has been interpreted as energy loss of the energetic partons traversing the produced hot and dense medium [5]. At intermediate  $p_T$ , the degree of suppression depends on particle species. The spectra of baryons (protons and lambdas) are less suppressed than those of mesons (pions, kaons) [6, 7] in the  $p_T$  range  $2 < p_T < 5$  GeV/c. The baryon content in the hadrons at intermediate  $p_T$  depends strongly on the impact parameter (centrality) of the Au+Au collisions with about 40% of the hadrons being baryons in the minimum-bias collisions and 20% in very peripheral collisions [6, 7]. Hydrodynamics [8, 9], parton coalescence at hadronization [10, 11, 12] and gluon junctions [13] have been suggested as explanations for the observed particle-species dependence.

On the other hand, the hadron  $p_T$  spectra have been observed to depend on the target atomic weight ( $A$ ) and the produced particle species in lower energy p+A collisions [14, 15, 16]. This is known as the “Cronin Effect”, a generic term for the experimentally observed broadening of the transverse momentum distributions at intermediate  $p_T$  in p+A collisions as compared to those in p+p collisions [14, 15, 16, 17, 18]. The effect can be characterized as a dependence of the yield on the target atomic weight as  $A^\alpha$ . At energies of  $\sqrt{s} \simeq 30$  GeV,  $\alpha$  depends on  $p_T$  and is greater than unity at high  $p_T$  [14, 15], indicating an enhancement of the production cross section. The effect has been interpreted as partonic scatterings at the initial impact [17, 18]. Thus, the Cronin effect is predicted to be larger in central d+Au collisions than in d+Au peripheral collisions [19]. At higher energies, multiple parton collisions are possible even in p+p collisions [20]. This combined with the hardening of the spectra with increasing beam energy would reduce the Cronin effect [18]. At sufficiently high beam energy, gluon saturation is expected to result in a relative suppression of hadron yield at high  $p_T$  in both p+A and A+A collisions and in a substantial decrease and finally in the disappearance of the Cronin effect [21].

Recent results on inclusive hadron production from d+Au collisions indicate that hadron suppression at intermediate  $p_T$  in Au+Au collisions is due to final-state effects [4, 22, 23]. The rapidity dependence of the particle yield at intermediate  $p_T$  shows suppression in forward rapidity (deuteron side) and enhancement in the backward rapidity (Au side) in d+Au collisions at RHIC [24, 25]. A study of particle composition will help understand the origin of the rapidity asymmetry [10]. In order to further understand the mechanisms responsible for the particle dependence of  $p_T$  spectra in heavy ion collisions, and to separate the effects of initial and final partonic rescatter-

ings, we measured the  $p_T$  distributions of  $\pi^\pm$ ,  $K^\pm$ ,  $p$  and  $\bar{p}$  from 200 GeV d+Au and p+p collisions. In this letter, we discuss the dependence of particle production on  $p_T$ , collision energy, and target atomic weight.

The detector used for these studies was the Solenoidal Tracker at RHIC (STAR). The main tracking device is the Time Projection Chamber (TPC) which provides momentum information and particle identification for charged particles up to  $p_T \sim 1.1$  GeV/c by measuring their ionization energy loss ( $dE/dx$ ) [26]. Detailed descriptions of the TPC and d+Au run conditions have been presented in Ref. [22, 26]. A prototype time-of-flight detector (TOFr) based on multi-gap resistive plate chambers (MRPC) [27] was installed in STAR for the d+Au and p+p runs. It extends particle identification up to  $p_T \sim 3$  GeV/c for  $p$  and  $\bar{p}$ . In p+p and d+Au collisions, the  $dE/dx$  resolution from TPC was found to be better than 8% and there is  $2 \sim 3\sigma$  separation between the  $dE/dx$  of pions at relativistic rise and the  $dE/dx$  of kaons and protons at  $p_T \gtrsim 2$  GeV/c [26]. By combining the particle identification capability of  $dE/dx$  from TPC and Time-of-Flight from TOFr, we are able to extend pion identification to  $\sim 3$  GeV/c [26, 28]. MRPC technology was first developed by the CERN ALICE group [29] to provide a cost-effective solution for large-area time-of-flight coverage.

TOFr covers  $\pi/30$  in azimuth and  $-1 < \eta < 0$  in pseudorapidity at a radius of  $\sim 220$  cm. It contains 28 MRPC modules which were partially instrumented during the 2003 run. Only particles from  $-0.5 < \eta < 0$  are selected where most of the MRPC modules were instrumented. Each module [27] is a stack of resistive glass plates with six uniform gas gaps. High voltage is applied to electrodes on the outer surfaces of the outer plates. A charged particle traversing a module generates avalanches in the gas gaps which are read out by 6 copper pickup pads with pad dimensions of  $31.5 \times 63$  mm $^2$ . The MRPC modules were operated at 14 kV with a mixture of 95%  $C_2H_2F_4$  and 5% iso-butane at 1 atmosphere. In d+Au collisions, TOFr is situated in the outgoing Au beam direction which is assigned negative  $\eta$ . The average MRPC TOFr timing resolution alone for the ten modules used in this analysis was measured to be 85 ps for both d+Au and p+p collisions. The “start” timing was provided by two identical pseudo-vertex position detectors (pVPD), each 5.4 m away from the TPC center along the beamline [30]. Each pVPD consists of 3 detector elements and covers  $\sim 19\%$  of the total solid angle in  $4.4 < |\eta| < 4.9$  [30]. Due to the low multiplicity in d+Au and p+p collisions, the effective timing resolution of the pVPDs was 85 ps and 140 ps, respectively.

Since the acceptance of TOFr is small, a special trigger selected events with a valid pVPD coincidence and at least one TOFr hit. A total of 1.89 million and 1.08 million events were used for the analysis from TOFr triggered d+Au and non-singly diffractive (NSD) p+p collisions, representing an integrated luminosity of about 40  $\mu b^{-1}$  and 30 nb $^{-1}$ , respectively. The d+Au minimum-

---

\*URL: [www.star.bnl.gov](http://www.star.bnl.gov)

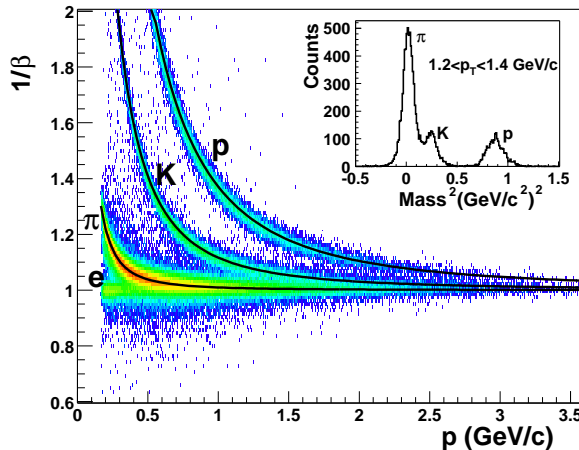


FIG. 1:  $1/\beta$  vs. momentum for  $\pi^\pm$ ,  $K^\pm$ , and  $p(\bar{p})$  from 200 GeV d+Au collisions. Separations between pions and kaons, kaons and protons are achieved up to  $p_T \simeq 1.6$  and 3.0 GeV/c, respectively. The insert shows  $m^2 = p^2(1/\beta^2 - 1)$  for  $1.2 < p_T < 1.4$  GeV/c. Clear separation of pions, kaons and protons is seen.

bias trigger required an equivalent energy deposition of about 15 GeV in the Zero Degree Calorimeter in the Au beam direction [22]. Minimum-bias p+p events were triggered by the coincidence of two beam-beam counters (BBC) covering  $3.3 < |\eta| < 5.0$  [1]. The NSD cross section was measured to be  $30.0 \pm 3.5$  mb by a van der Meer scan and PYTHIA [31] simulation of the BBC acceptance [1]. A small multiplicity bias ( $\lesssim 10\%$  in d+Au and 18% in p+p) at mid-rapidity was observed in TOFr triggered events due to the further pVVD trigger requirement and was corrected for using minimum-bias data sets and PYTHIA [31] and HIJING [32] simulations. The effect of the trigger bias on the mid-rapidity particle spectra was found to be independent of particle  $p_T$  at  $p_T > 0.3$  GeV/c [33]. Centrality tagging of d+Au collisions was based on the charged particle multiplicity in  $-3.8 < \eta < -2.8$ , measured by the Forward Time Projection Chamber in the Au beam direction [22, 34]. The TOFr triggered d+Au events were divided into three centralities: most central 20%, 20 – 40% and 40 –  $\sim 100\%$  of the hadronic cross section. The average number of binary collisions  $\langle N_{bin} \rangle$  for each centrality class and for the combined minimum-bias event sample is derived from Glauber model calculations and listed in Table I.

The TPC and TOFr are two independent systems. In the analysis, hits from particles traversing the TPC were reconstructed as tracks with well defined geometry, momentum, and  $dE/dx$  [26]. The particle trajectory was then extended outward to the TOFr detector plane. Fig. 1 shows inverse velocity ( $1/\beta$ ) from TOFr measurement as a function of momentum ( $p$ ) calculated from TPC tracking in TOFr triggered d+Au collisions. The raw yields of  $\pi^\pm$ ,  $K^\pm$ ,  $p$  and  $\bar{p}$  are obtained from Gaussian fits to the distributions in  $m^2 = p^2(1/\beta^2 - 1)$  in each  $p_T$  bin. For  $\pi^\pm$  at  $p_T > 1.8$  GeV/c, an additional cut on  $dE/dx$  was applied at 50% efficiency [28]. The  $dE/dx$  distribution was measured by selecting on

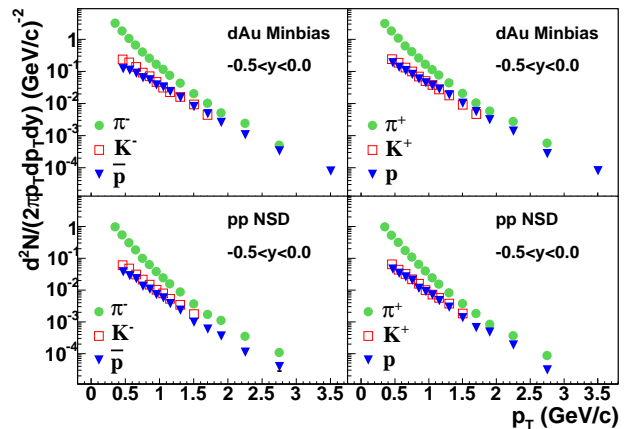


FIG. 2: The invariant yields of  $\pi^+$  (filled circles),  $K^+$  (open squares),  $p$  (filled triangles) and their anti-particles as a function of  $p_T$  from d+Au and NSD p+p events at 200 GeV. The rapidity range was  $-0.5 < y < 0.0$  with the direction of the outgoing Au ions as negative rapidity. Errors are statistical.

pure pion and proton samples from TOFr. The uncertainty of this cut was evaluated by systematically studying the yield as a function of the cut. Acceptance and efficiency were studied by Monte Carlo simulations and by matching TPC track and TOFr hits in real data. TPC tracking and MRPC hit matching efficiencies were both about 90%. Weak-decay feeddown (e.g.  $K_s^0 \rightarrow \pi^+\pi^-$ ) to pions is  $\sim 12\%$  at  $p_T < 1$  GeV/c and  $\sim 5\%$  at higher  $p_T$ , and was corrected for using PYTHIA [31] and HIJING [32] simulations. Inclusive  $p$  and  $\bar{p}$  production is presented without hyperon feeddown correction.  $p$  and  $\bar{p}$  from hyperon decays have the same detection efficiency as primary  $p$  and  $\bar{p}$  [35] and contribute about 20% to the inclusive  $p$  and  $\bar{p}$  yield, as estimated from the simulation.

The invariant yields  $d^2N/(2\pi p_T dp_T dy)$  of  $\pi^\pm$ ,  $K^\pm$ ,  $p$  and  $\bar{p}$  from both NSD p+p and minimum-bias d+Au events are shown in Fig. 2. The average bin-to-bin systematic uncertainty was estimated to be of the order of 8%. The systematic uncertainty is dominated by the uncertainty in the detector response in Monte Carlo simulations ( $\pm 7\%$ ). The normalization uncertainties in d+Au minimum-bias and p+p NSD collisions are 10% and 14%, respectively [1, 22]. The charged pion yields are consistent with  $\pi^0$  yields measured by the PHENIX collaboration in the overlapping  $p_T$  range [2, 23].

Nuclear effects on hadron production in d+Au collisions are measured through comparison to the p+p spectrum, scaled by the number of underlying nucleon-nucleon inelastic collisions using the ratio

$$R_{dAu} = \frac{d^2N/(2\pi p_T dp_T dy)}{T_{dAu} d^2\sigma_{inel}^{pp} / (2\pi p_T dp_T dy)},$$

where  $T_{dAu} = \langle N_{bin} \rangle / \sigma_{inel}^{pp}$  describes the nuclear geometry, and  $d^2\sigma_{inel}^{pp} / (2\pi p_T dp_T dy)$  for p+p inelastic collisions is derived from the measured p+p NSD cross section. The difference between NSD and inelastic differ-

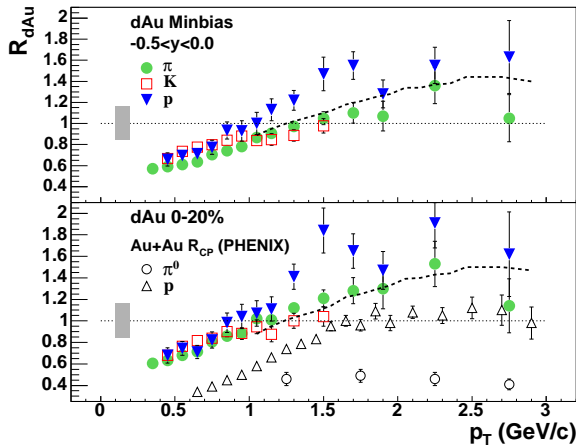


FIG. 3: The identified particle  $R_{dAu}$  for minimum-bias and top 20% d+Au collisions. The filled triangles are for  $p + \bar{p}$ , the filled circles are for  $\pi^+ + \pi^-$  and the open squares are for  $K^+ + K^-$ . Dashed lines are  $R_{dAu}$  of inclusive charged hadrons from [22]. The open triangles and open circles are  $R_{CP}$  of  $p + \bar{p}$  and  $\pi^0$  in Au+Au collisions measured by PHENIX [7]. Errors are statistical. The gray band represents the normalization uncertainty of 16%.

ential cross sections at mid-rapidity, as estimated from PYTHIA [31], is 5% at low  $p_T$  and negligible at  $p_T > 1.0$  GeV/c. Fig. 3 shows  $R_{dAu}$  of  $\pi^+ + \pi^-$ ,  $K^+ + K^-$  and  $p + \bar{p}$  for minimum-bias and central d+Au collisions. The systematic uncertainties on  $R_{dAu}$  are of the order of 16%, dominated by the uncertainty in normalization. The  $R_{dAu}$  of the same particle species are similar between minimum-bias and top 20% d+Au collisions. In both cases, the  $R_{dAu}$  of protons rise faster than  $R_{dAu}$  of pions and kaons. We observe that the spectra of  $\pi^\pm$ ,  $K^\pm$ ,  $p$  and  $\bar{p}$  are considerably harder in d+Au than those in p+p collisions.

The  $R_{dAu}$  of the identified particles has characteristics of the Cronin effect [14, 15, 16, 18] in particle production with  $R_{dAu}$  less than unity at low  $p_T$  and above unity at  $p_T > 1.0$  GeV/c. On the contrary, the  $R_{CP}$  (nuclear modification factor between central and peripheral collisions) of identified particles in Au+Au collisions at  $\sqrt{s_{NN}} = 200$  GeV as measured by PHENIX and STAR collaborations [6, 7] do not have the above features. The  $R_{CP}$  of  $p + \bar{p}$  follows binary scaling and that of  $\pi^0$  shows large suppression of meson production in central Au+Au collisions [7] as depicted in the bottom panel of Fig. 3. It is notable that the  $R_{dAu}$  of proton and anti-proton are greater than unity in both central and minimum-bias d+Au collisions while the proton and antiproton production follows binary scaling in all centralities in Au+Au collisions [7].

Fig. 4 depicts  $(p + \bar{p})/h$ , the ratio of protons ( $p + \bar{p}$ ) over inclusive charged hadrons ( $h$ ) as a function of  $p_T$  in d+Au and p+p minimum-bias collisions at  $\sqrt{s_{NN}} = 200$  GeV, and Au+Au minimum-bias collisions at  $\sqrt{s_{NN}} = 130$  GeV [7]. The systematic uncertainties on these ratios were estimated to be of the order of 10% for  $p_T \lesssim 1.0$

TABLE I:  $\langle N_{bin} \rangle$  from a Glauber model calculation,  $(p + \bar{p})/h$  averaged over the bins within  $1.2 < p_T < 2.0$  GeV/c (left column) and within  $2.0 < p_T < 3.0$  GeV/c (right column) and the  $R_{dAu}$  ratios between  $p + \bar{p}$  and  $h$  averaged over  $1.2 < p_T < 3.0$  GeV/c for minimum-bias, centrality selected d+Au collisions and minimum-bias p+p collisions. A p+p inelastic cross section of  $\sigma_{inel} = 42$  mb was used in the calculation. For  $R_{dAu}$  ratios, only statistical errors are shown and the systematic uncertainties are 0.03 for all centrality bins.

centrality	$\langle N_{bin} \rangle$	$(p + \bar{p})/h$	$R_{dAu}^{p+\bar{p}}/R_{dAu}^h$
min. bias	$7.5 \pm 0.4$	$0.21 \pm 0.01$	$0.24 \pm 0.01$
0-20%	$15.0 \pm 1.1$	$0.21 \pm 0.01$	$0.24 \pm 0.02$
20-40%	$10.2 \pm 1.0$	$0.20 \pm 0.01$	$0.24 \pm 0.02$
40-~100%	$4.0^{+0.8}_{-0.3}$	$0.20 \pm 0.01$	$0.23 \pm 0.02$
p+p	1.0	$0.17 \pm 0.01$	$0.21 \pm 0.02$
			—

GeV/c, decreasing to 3% at higher  $p_T$ . At RHIC energies, the anti-particle to particle ratios approach unity ( $\bar{p}/p = 0.81 \pm 0.02 \pm 0.04$  in d+Au minimum-bias collisions) and their nuclear modification factors are similar. The  $(p + \bar{p})/h$  ratio from minimum-bias Au+Au collisions [7] at a similar energy is about a factor of 2 higher than that in d+Au and p+p collisions for  $p_T \gtrsim 2.0$  GeV/c. This enhancement is most likely due to final-state effects in Au+Au collisions [5, 8, 9, 11, 12, 13]. The ratios show little centrality dependence in d+Au collisions, as shown in Table I. The identified particle yields can also provide important information and constraints for other studies even when our measurements are in a limited rapidity range ( $-0.5 < y < 0.0$ ). Our measurement of  $(p + \bar{p})/h$  ratio shows that baryons account for only about 20% of the total inclusive charged hadrons with little centrality dependence. Therefore, the measurement of rapidity asymmetry of inclusive charged hadrons around mid-rapidity by the STAR collaboration [24] is unlikely due to a change in particle composition or baryon stopping. For  $p_T < 2.0$  GeV/c, the  $(p + \bar{p})/h$  ratio in p+ $\bar{p}$  collisions at  $\sqrt{s_{NN}} = 1.8$  TeV [36] is very similar to those in d+Au and p+p collisions at  $\sqrt{s_{NN}} = 200$  GeV. Also shown are  $p/h^+$  ratios in p+p and p+W minimum-bias collisions at  $\sqrt{s_{NN}} = 23.8$  GeV [14, 15]. Although the relative yields of particles and anti-particles are very different, the Cronin effects are similar. At  $\sqrt{s} < 40$  GeV, there is a general trend of decreasing Cronin effect of all particles with beam energies at high  $p_T$  [15, 16], however, the Cronin effects of  $\bar{p}$  data are less conclusive [16].

The difference between  $R_{dAu}$  at  $\sqrt{s_{NN}} = 200$  GeV for  $p + \bar{p}$  and  $h$  can be obtained from the  $(p + \bar{p})/h$  ratios in d+Au and p+p collisions. Table I shows  $R_{dAu}^{p+\bar{p}}/R_{dAu}^h$  determined by averaging over the bins within  $1.2 < p_T < 3.0$  GeV/c. Alternatively, we can study Cronin effect of the identified particles by comparing the  $\alpha$  parameters of protons and pions. At lower energy, the  $\alpha$  parameter in the power law dependence on target atomic weight  $A^\alpha$  of identified particle production falls with  $\sqrt{s}$  [15, 16] at high  $p_T$  ( $p_T \simeq 4.6$  GeV/c). From the ratios of  $R_{dAu}$  between  $p + \bar{p}$  and  $\pi^+ + \pi^-$ , we may fur-

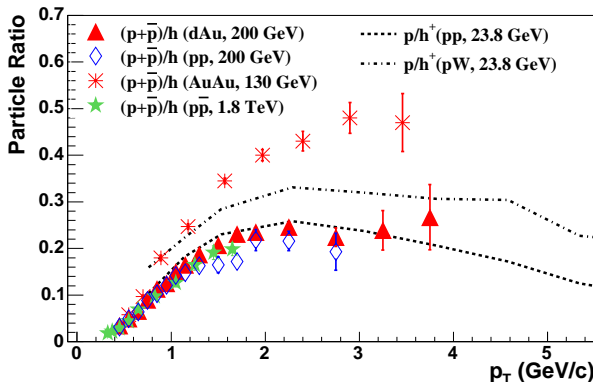


FIG. 4: Minimum-bias ratios of protons ( $p + \bar{p}$ ) over inclusive charged hadrons ( $h$ ) at  $-0.5 < \eta < 0.0$  from  $\sqrt{s_{NN}} = 200$  GeV p+p (open diamonds), d+Au (filled triangles) and  $\sqrt{s_{NN}} = 130$  GeV Au+Au [7] (asterisks) collisions. Results of  $p + \bar{p}$  collisions at  $\sqrt{s_{NN}} = 1.8$  TeV [36] are shown as solid stars. Dashed lines are results of  $p/h^+$  ratios from  $\sqrt{s_{NN}} = 23.8$  GeV p+p (short-dashed lines) and p+W (dot-dashed) collisions [14, 15]. Errors are statistical.

ther derive the  $\alpha_{p+\bar{p}} - \alpha_{\pi^+ + \pi^-}$  for  $1.2 < p_T < 3.0$  GeV/c to be  $0.048 \pm 0.012(\text{stat}) \pm 0.006(\text{syst})$ . This result is significantly smaller than the value  $0.081 \pm 0.005$  in the same  $p_T$  range found at lower energies [15].

In summary, we have reported the identified particle spectra of pions, kaons, and protons at mid-rapidity from 200 GeV p+p and d+Au collisions. The time-of-flight detector, based on novel multi-gap resistive plate chamber technology, was used for particle identification. The particle-species dependence of the Cronin effect is found to be significantly smaller than that from lower energy

p+A collisions. In  $\sqrt{s_{NN}} = 200$  GeV d+Au collisions, the ratio of the nuclear modification factor  $R_{dAu}$  between protons ( $p + \bar{p}$ ) and inclusive charged hadrons ( $h$ ) in the  $p_T$  range  $1.2 < p_T < 3.0$  GeV/c was measured to be  $1.19 \pm 0.05(\text{stat}) \pm 0.03(\text{syst})$  in minimum-bias collisions. Both the  $R_{dAu}$  values and  $(p + \bar{p})/h$  ratios show little centrality dependence, in contrast to previous measurements in Au+Au collisions at  $\sqrt{s_{NN}} = 130$  and 200 GeV. The ratios of protons over inclusive charged hadrons in d+Au and p+p collisions are found to be about a factor of 2 lower than that from Au+Au collisions, indicating that the Cronin effect alone is not enough to account for the relative baryon enhancement observed in heavy ion collisions.

The STAR Collaboration gratefully acknowledges the pioneering research and development work performed by LAA project, and especially C. Williams, under A. Zichichi on MRPC Time of Flight Technology. We thank the RHIC Operations Group and RCF at BNL, and the NERSC Center at LBNL for their support. This work was supported in part by the HENP Divisions of the Office of Science of the U.S. DOE; the U.S. NSF; the BMBF of Germany; IN2P3, RA, RPL, and EMN of France; EPSRC of the United Kingdom; FAPESP of Brazil; the Russian Ministry of Science and Technology; the Ministry of Education and the NNSFC of China; Grant Agency of the Czech Republic, FOM of the Netherlands, DAE, DST, and CSIR of the Government of India; Swiss NSF; the Polish State Committee for Scientific Research; and the STAA of Slovakia.

---

[1] STAR Collaboration, J. Adams *et al.*, Phys. Rev. Lett. **91**, 172302 (2003).  
[2] PHENIX Collaboration, S.S. Adler *et al.*, Phys. Rev. Lett. **91**, 072301 (2003); PHENIX collaboration, S.S. Adler *et al.*, Phys. Rev. Lett. **91**, 241803 (2003).  
[3] PHOBOS Collaboration, B.B. Back *et al.*, Phys. Lett. B **578**, 297 (2004).  
[4] BRAHMS Collaboration, I. Arsene *et al.*, Phys. Rev. Lett. **91**, 072305 (2003).  
[5] M. Gyulassy *et al.*, Review for: Quark Gluon Plasma 3, Editors: R.C. Hwa and X.N. Wang, World Scientific, Singapore, nucl-th/0302077.  
[6] STAR Collaboration, J. Adams *et al.*, Phys. Rev. Lett. **92**, 052302 (2004).  
[7] PHENIX Collaboration, K. Adcox *et al.*, Phys. Lett. B **561**, 82 (2003); PHENIX Collaboration, S.S. Adler *et al.*, Phys. Rev. Lett. **91**, 172301 (2003).  
[8] D. Teaney *et al.*, nucl-th/0110037; D. Teaney *et al.*, Phys. Rev. Lett. **86**, 4783 (2001).  
[9] P. Huovinen, Nucl. Phys. A **715**, 299c (2003).  
[10] R.C. Hwa *et al.*, Phys. Rev. C **67**, 034902 (2003); R.C. Hwa *et al.*, nucl-th/0410111.  
[11] R.J. Fries *et al.*, Phys. Rev. C **68**, 044902 (2003).  
[12] V. Greco *et al.*, Phys. Rev. Lett. **90**, 202302 (2003).  
[13] I. Vitev and M. Gyulassy, Phys. Rev. C **65**, 041902 (2002).  
[14] J.W. Cronin *et al.*, Phys. Rev. Lett. **31**, 1426 (1973); J.W. Cronin *et al.*, Phys. Rev. D **11**, 3105 (1975).  
[15] D. Antreasyan *et al.*, Phys. Rev. D **19**, 764 (1979).  
[16] P.B. Straub *et al.*, Phys. Rev. Lett. **68**, 452 (1992).  
[17] M. Lev and B. Petersson, Z. Phys. C **21**, 155 (1983).  
[18] A. Accardi, Contribution to the CERN Yellow report on Hard Probes in Heavy Ion Collisions at the LHC, hep-ph/0212148; X.N. Wang, Phys. Rev. C **61**, 064910 (2000).  
[19] I. Vitev, Phys. Lett. B **562**, 36 (2003).  
[20] T. Alexopoulos *et al.*, Phys. Lett. B **435**, 453 (1998).  
[21] D. Kharzeev *et al.*, Phys. Lett. B **561**, 93 (2003); J. Jalilian-Marian *et al.*, Phys. Lett. B **577**, 54 (2003); J.L. Albacete *et al.*, Phys. Rev. Lett. **92**, 082001 (2004); D. Kharzeev *et al.*, Phys. Rev. D **68**, 094013 (2003); R. Baier *et al.*, Phys. Rev. D **68**, 054009 (2003).  
[22] STAR Collaboration, J. Adams *et al.*, Phys. Rev. Lett. **91**, 072304 (2003).  
[23] PHENIX Collaboration, S.S. Adler *et al.*, Phys. Rev. Lett. **91**, 072303 (2003); PHOBOS Collaboration, B.B. Back *et al.*, Phys. Rev. Lett. **91**, 072302 (2003).  
[24] STAR Collaboration, J. Adams *et al.*, Phys. Rev. C **70**, 064907 (2004).  
[25] PHOBOS Collaboration, B.B. Back *et al.*, Phys. Rev. C

**70**, 061901 (2004).

[26] M. Anderson *et al.*, Nucl. Instr. Meth. A **499**, 659 (2003).

[27] B. Bonner *et al.*, Nucl. Instr. Meth. A **508**, 181 (2003); M. Shao *et al.*, Nucl. Instr. Meth. A **492**, 344 (2002).

[28] STAR Collaboration, M. Shao *et al.*, The Proceedings of Hot Quarks 2004, to be published in Journal of Physics G, nucl-ex/0411035.

[29] E. Cerron Zeballos *et al.*, Nucl. Instr. Meth. A **374**, 132 (1996); M.C.S. Williams *et al.*, Nucl. Instr. Meth. A **478**, 183 (2002).

[30] W.J. Llope *et al.*, Nucl. Instr. Meth. A **522**, 252 (2004).

[31] T. Sjöstrand, P. Eden, C. Friberg *et al.*, Comput. Phys. Commun. **135**, 238 (2001).

[32] X.N. Wang and M. Gyulassy, Phys. Rev. D **44**, 3501 (1991).

[33] Lijuan Ruan, Ph.D. thesis, University of Science and Technology of China, 2004, nucl-ex/0503018.

[34] K.H. Ackermann *et al.*, Nucl. Instr. Meth. A **499**, 713 (2003).

[35] STAR Collaboration, C. Adler *et al.*, Phys. Rev. Lett. **87**, 262302 (2001); STAR Collaboration, J. Adams *et al.*, Phys. Rev. Lett. **92**, 112301 (2004).

[36] T. Alexopoulos *et al.*, Phys. Rev. D **48**, 984 (1993).